Composites Science and Technology 146 (2017) 1–9

Contents lists available at ScienceDirect

Composites Science and Technology

journal homepage: http://www.elsevier.com/locate/compscitech

# Damping of carbon fibre and flax fibre angle-ply composite laminates

M. Rueppel [a, **], J. Rion [b], C. Dransfeld [a], C. Fischer [b], K. Masania [c, *]

[a] Institute of Polymer Engineering, FHNW University of Applied Sciences and Arts Northwestern Switzerland, CH-5210, Windisch, Switzerland
[b] Bcomp AG, CH-1700, Fribourg, Switzerland
[c] Complex Materials, Department of Materials, ETH Zurich, CH-8093, Zurich, Switzerland

ARTICLE INFO

*Article history:*
Received 8 August 2016
Received in revised form
30 March 2017
Accepted 8 April 2017
Available online 12 April 2017

*Keywords:*
Natural fibres
Layered structures
Vibration
Elastic properties
Dynamic mechanical thermal analysis (DMTA)

ABSTRACT

The damping behaviour of continuous carbon fibre and flax fibre reinforced polymer (CFRP and FFRP) composites was studied by comparing angle-ply laminates. Using logarithmic decrement measurements, dynamic mechanical analysis and vibration beam measurements, the damping was described as the specific damping capacity $\psi$ in order to compare data using the different methods.

Our results show approximately 2–3 times better damping of FFRP compared to CFRP at low frequency and low strain. We show that the damping of both materials increases with increasing angle-ply orientation below 300 Hz. While the matrix and interface seems to contribute mainly to damping at lower frequencies, the fibre shows an increasing contribution with $\psi = 64.4\%$ for unidirectional FFRP at 1259 Hz in the 5*th* mode of vibration, without a notable change in the elastic modulus. This work demonstrates that the FFRP may be simultaneously stiff and efficient at damping.



## 1. Introduction

The high specific elastic modulus and specific strength of carbon fibre reinforced polymer composites (CFRPs) make them attractive for lightweight applications. Lightweight structures are however, prone to vibrations which lead to unwanted instability, reduced efficiency or in severe cases, structural failure. This can lead to conservative design, or the need of additional vibration damping which adds weight.

Flax fibre reinforced polymer composites (FFRPs) have gained interest due to their low environmental footprint and relatively good specific mechanical properties [1]. In flax fibres, semi-crystalline cellulose microfibrils are embedded in pectin and hemicellulose matrix [2]. These are ordered into cell walls enclosing a lumen to form the fibre microstructure. Stiffness and strength is primarily given by the secondary wall, ordered with an acute angle of 10° to the fibre direction. In turn, these elementary fibres are bundled with a lignin matrix and twisted together to form the structural fibre [3]. The combination of stiff discontinuous fibres connected with soft matrices means that such hierarchical flax fibre-epoxy composites have an order of magnitude higher damping than aluminium and exhibit three times higher damping than carbon- or glass-fibre composites [4], making it a very attractive composite material to simultaneously provide structural damping and stiffness [5]. We build on this work by studying the effect of frequency and strain on FFRPs.

Several effects need to be considered to describe the damping behavior of such hierarchical composite materials. Fibre deformation [6], interphase viscoelasticity [7], matrix modification [8], columb friction at the interface [9], moisture, temperature [10] and ply angle are known to contribute to the overall damping [11]. Known methods to reduce and shift eigenmodes in composites have included viscoelastic layers [12], bolting or joining of structures [13], and damage or delamination [14], which add weight and/or are undesired. Previous works show that damping experiments can provide trends, but do not always yield comparable quantitative results due the test set up, excitation and material interaction across length scales. We aim to compare damping across sample size, excitation frequencies and applied strain by reducing the measurements to a common damping description, the specific damping capacity.

The specific damping capacity $\psi$ may be defined as

$$\psi = \frac{\Delta U}{U} \tag{1}$$

* Corresponding author.
** Corresponding author.
*E-mail addresses:* marvin.rueppel@fhnw.ch (M. Rueppel), kunal.masania@mat.ethz.ch (K. Masania).

http://dx.doi.org/10.1016/j.compscitech.2017.04.011
0266-3538/

where $\Delta U$ is the total energy loss per cycle and $U$ is the maximum elastic stored energy [11]. This measure is useful as its energy definition is applicable to any damping measurement method.

## 2. Materials

Carbon fibre reinforced polymer composites were produced from unidirectional pre-preg Toray M40JB fibre ThinPreg TM 80EP-736/CF with an areal weight of 30 g/m$^2$ (North Thin Ply Technology, Switzerland, [15]). Unidirectional non-crimp flax fibre fabric with an areal weight of 300g/m$^2$, type 5009 (Bcomp AG, Switzerland) with a twist angle of 20°, was used in combination with ThinPreg TM 80EP-736 (North Thin Ply Technology, Switzerland) epoxy matrix for consistency in our measurements.

The CFRPs were produced with 80 layers of 0.03 mm prepreg and FFRP composites were produced with 8 layers of 0.3 mm to produce lay ups with angle-ply orientations of 0°, ±10°, ±20°, ±30°, ±60° and 90° resulting in approximately 2.4 – 2.5 mm thick laminates. The composites were prepared (after a flax fibre pre-drying process of 110° C for 30 min) using autoclave manufacturing for the CFRP or compression resin transfer moulding for the FFRP and cured at 100° C for 2 h using a pressure of 1 MPa. Subsequent differential scanning calorimetry was used to ensure that the composites were indeed fully cured with a glass transition temperature of 115°C and optical microscopy of polished cross sections confirmed a porosity of less than 2 % in the water-jet cut samples. All of the samples were dried at 40°C in a vacuum overnight prior to testing.

## 3. Experimental methodology

Three measurement methods were studied to characterise the damping behaviour of FFRP with CFRP as a reference material for comparison, as shown in Table 1. The logarithmic decrement measurement method (LDM) measures the decay of vibration of a beam oscillating at its natural frequency $f_n$. Dynamic mechanical analysis (DMA) was performed to provide a clamp free measurement using the non-resonant damping experiment. Lastly, vibration beam measurements (VBM) were conducted to allow measurement of resonant damping at very large amplitudes, identify many modes of vibration and the study of a broad frequency range. The dynamic behaviour, elastic modulus $E$ was derived using these methods, then damping was related to the specific damping capacity $\psi$ in order to compare damping in CFRP and FFRP composites.

### 3.1. Logarithmic decrement measurement

The logarithmic decrement $\delta$ is a damping measure for linear systems in the time domain. The test was performed on beams of vibrating length $L = 290$ mm, declining at their natural frequency $f_n$ from a pre-defined deflection. The specimens were clamped at one end with a fixed torque of 15 Nm. A fixed displacement $X_0 = 5$ mm was applied to a point $l = 150$ mm along the beam and then the decline in amplitude was recorded as a function of time using an OptoNCDT 1700 Laser displacement sensor. Two samples were tested from a single plate and each sample was removed and re-clamped until three repeat measurements were obtained for each material (total six tests). Typically, an exponential function may be fit to the recorded amplitude decay in order to describe the vibration decline. Additionally, one may analyse the Fourier spectra to obtain the natural frequencies and damping via the quality factor Q which is the reciprocal of the dimensionless bandwidth, that describes the magnitude of under-damping of the system in resonance [16].

**Table 1**
Properties of the damping measurement methods studied.

| Method | Sample size | Frequency | Clamping torque | Measure |
|---|---|---|---|---|
| LDM | $360 \times 45$mm$^2$ | $f_n$ | 15 Nm | $\delta$ |
| DMA | $60 \times 10$mm$^2$ | 0.1–100 Hz | – | tan($\gamma$) |
| VBM | $360 \times 45$mm$^2$ | 5-3000 Hz | 15 Nm | Q factor |

For linear under-damped systems in the time domain, defined by a parallel spring-damper material model with an attached mass $m$

$$0 = m\ddot{x}(t) + c\dot{x}(t) + kx(t) \tag{2}$$

where $c$ is the damper coefficient and $k$ is the spring constant. The solution $x(t)$ to (2) is

$$x(t) = X_0 exp(-\tau t)\cos(T\,t) \tag{3}$$

with the initial displacement $X_0$, the decline rate $\tau$ and the period $T$. The decrement $\delta$ for a one dimensional decline can be determined by the decline of a free vibrating beam from one maximum amplitude $\widehat{x}(t)$, to the next $\widehat{x}(t+T)$ [17].

$$\delta := \ln \frac{\widehat{x}(t)}{\widehat{x}(t+T)} \tag{4}$$

with the period $T = 1/f_n$ the eigenfrequency $f_n$ the decay rate $\tau$ and time $t$. Using (3), the decrement becomes

$$\delta = \ln \frac{X_0 exp(-\tau t)}{X_0 exp(-\tau(t+T))} = \tau T = \frac{\tau}{f_n} \tag{5}$$

Further, solving the following system of equations, one may convert $\delta$ to the specific damping capacity $\psi$.

$$\zeta = \frac{\delta}{\sqrt{4\pi^2 + \delta^2}} \tag{6}$$

$$Q^{-1} = \sqrt{\left(1 - 2\zeta^2 + 2\zeta\sqrt{1+\zeta^2}\right)} - \sqrt{\left(1 - 2\zeta^2 - 2\zeta\sqrt{1+\zeta^2}\right)} \tag{7}$$

$$Q^{-1} = \sqrt{1 + \frac{\psi}{2\pi}} - \sqrt{1 - \frac{\psi}{2\pi}} \tag{8}$$

Using Taylor expansions for $\delta$ close to zero, i.e. low damping, one may find the commonly used approximation $\psi_{LDM} \approx 2\delta$ [4]. Representative LDM measurements of 0° CFRP and FFRP in are shown in Fig. 1. The time domain envelopes of these measured declining vibrations did not follow the one dimensional linear vibration posed by equation (2). When analysing the Fourier spectra, more than one resonance frequency $f_n$ with notable and significant power was identified. As is evident in Fig. 1. Model (2) was therefore extended to a two dimensional space. The solution $x(t)$ and resulting envelope $g(t)$ of the free vibration becomes

$$x(t) = \sum_{i=1}^{2} c_i exp(-\tau_i t)\cos\left(\sqrt{\omega_{n_i}^2 - \tau_i^2}\; t\right) \tag{9}$$

$$g(t) = (c_1 exp(-\tau_1 t) + c_2 exp(-\tau_2 t)) \quad c_1 + c_2 = X_0 \tag{10}$$

The envelope $g(t)$ is the sum of the two exponential declines.

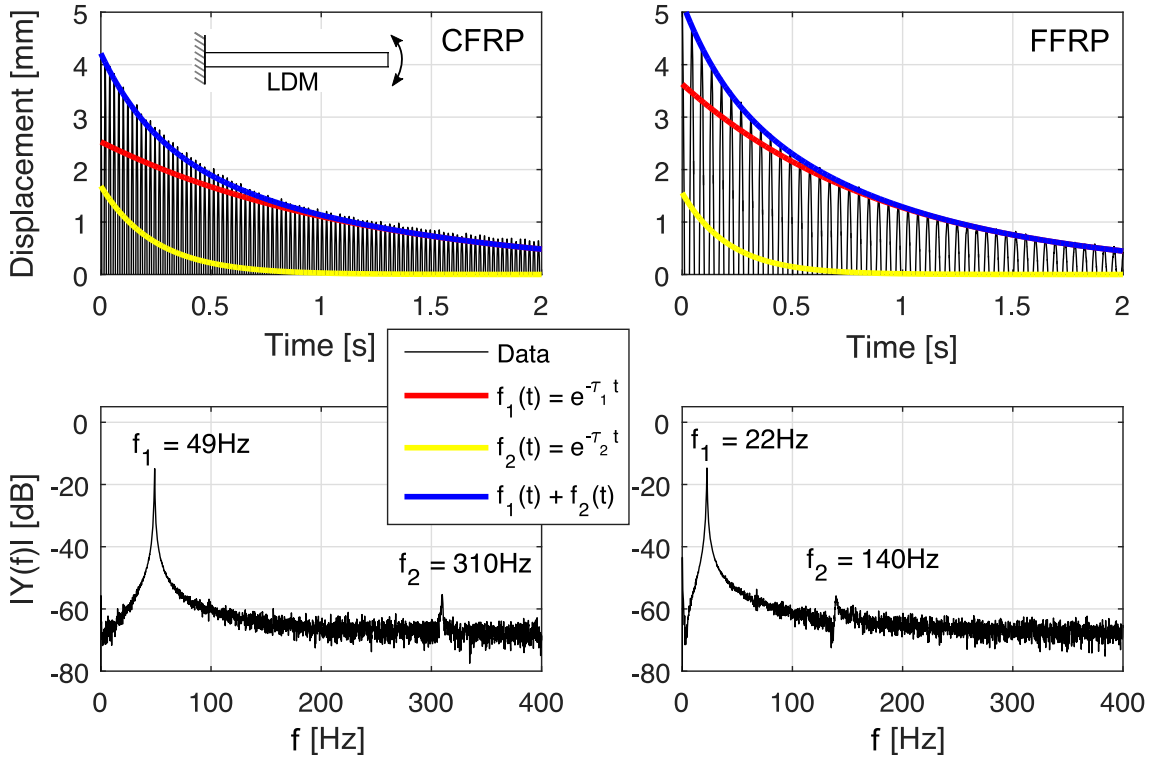


**Fig. 1.** Logarithmic decrement method (LDM) vibration of representative CFRP and FFRP angle-ply composites ($\pm\theta = 30^\circ$). Both of the studied composites decline with a sum of two frequencies $f_1$ and $f_2$, which sum to form the decline that was observed experimentally.

Conclusive damping values were not identified in time domain, thus the damping was determined by computing the Q factor in the Fourier Domain, which was then related to the specific damping capacity $\psi_{LDM}$ [18], using

$$\psi_{LDM_n} = 2\pi\sqrt{1-\frac{\left(2-\frac{1}{Q_n^2}\right)^2}{4}}, \quad Q_n := \frac{f_n}{f_{h_1}-f_{h_2}} \tag{11}$$

with the half power points $f_{h_i}$. Further, to find the elastic modulus $E_{LDM}$, the Euler beam equation was used

$$\frac{\delta^4 w}{\delta x^4} + \frac{\rho A}{EI_x}\frac{\delta^2 w}{\delta t^2} = \frac{F(x,t)}{EIx} \tag{12}$$

with the displacement $w$, area $A$, density $\rho$, second area moment of inertia $I_x$ and the force $F$. Euler beam theory was preferred over Timoshenko beam theory due to our low thickness to span ratio of 0.008, therefore transverse shear induced deformation was negligible. Equation (12) may be posed as an eigenvalue problem and the quotient $\frac{\rho A}{EI}$ is related to the resonance frequency of a beam [19]. This results in a relation between the elastic modulus $E_n$ at mode $n$ and resonance frequency $f_n$

$$E_{LDM_n} = \frac{\rho A(2\pi f_n)^2}{\beta_n^4 I_x} \tag{13}$$

with the beam length $L$ dependent parameter $\beta_n$ [19] which represents a mode shape dependant constant, allowing the measured resonance frequencies to be converted to a beam stiffness. Using (5), the decline $\tau_i$ can be calculated using data from the frequency domain,

$$\tau_i = \psi_i f_{n_i}/2 \tag{14}$$

as shown in Fig. 1, the two exponentials were found using the Fourier spectra and their addition showed a good fit to the observed decline, thus concluding that this was a preferable approach.

### 3.2. Dynamic mechanical analysis

The measurements were performed on a TA Instruments Q800 DMA using a three point bending set up at frequencies of 1 Hz and 25 Hz. The CFRP samples measured 60 mm by 6 mm and the FFRP samples measured 60 mm by 10 mm in order to generate more strain in the CFRP while respecting the force limit of the machine. A pre-load of 0.05 N was applied and the amplitude was set to 17 $\mu$m or 42 $\mu$m for CFRP and FFRP, respectively, with three samples for each material at a constant temperature of 30 °C, with each measurement repeated twice including remounting the sample, totalling six measurements.

The complex modulus **E** consisting of the storage modulus $E'$, the loss modulus $E''$ and the tangent of the complex moduli $\tan(\gamma) := \frac{E''}{E'}$, is based on the following forced vibration equation of motion

$$f(t) = m\ddot{x}(t) + \left(E' - iE''\right)x(t) \tag{15}$$

with the imaginary unit $i$. Physically, complex values in time domain are not interpretable [16], but are widely accepted in material damping because this usage simplifies the underlining equations. The relation of $\tan(\gamma)$ and (15) may be shown by computing the transfer function $H$ of system (15). The FT of (15) is

$$F(\omega) = X(\omega)\left(m\omega^2 + E' - i\omega E''\right) \tag{16}$$

with input $F(\omega) = \Im(f(t))$ and output $X(\omega) = \Im(x(t))$. The transfer function $H$ of (15) with the phase $\phi$ is

$$H(\omega) = \frac{1}{E' + m\omega^2 - i\omega E''} \quad \phi(\omega) = \arctan\left(\frac{-E''}{E' + m\omega^2}\right) \tag{17}$$

By neglecting the mass $m$ these equations reproduce the definition of $\tan(\gamma)$.

$$H(\omega) = \frac{1}{E' - i\omega E''} \quad \phi(\omega) = \arctan\left(\frac{E''}{E'}\right) = \gamma \tag{18}$$

Thus, the frequency dependent phase shift $\phi(\omega) = \gamma$, between the force input and the displacement output describes damping, assuming the mass of the sample is small. Summing $\gamma$ over a full cycle, $\psi_{DMA}$ may be written as

$$\psi_{DMA} := 2\pi\eta = 2\pi\tan(\phi(\omega)) \tag{19}$$

The elastic modulus $E_{DMA}$ was extracted from the complex modulus as

$$E_{DMA} = \Re(\mathbf{E}) = E' \tag{20}$$

### 3.3. Vibration beam measurement

Vibration beam tests were conducted on a Tira LS-340 shaker by clamping one end of the composite beam with a torque of 15 Nm. Accelerometers were mounted to the free edge and to the shaker. The accelerometer on the shaker was set as the master motor-control and an acceleration sine curve was performed for a frequency sweep from 5 Hz to 3 kHz. Sensor data was recorded on a Signal Star Vector, Dataphysics, which computed the Fourier transform of test beam. The maximum input acceleration varied from 0.75 g to 2 g, with $g = 9.81\ m/s^2$, in order to generate maximum tip displacements of about 150 mm. The tip displacement close to the $1^{st}$ mode of resonance frequency was set to approximately 150 mm by adjusting the acceleration. Then a frequency sweep was performed at constant acceleration to obtain the transfer function which was the input acceleration over the output acceleration at the beam tip. Extraneous sources of damping such as air damping and friction damping from specimen supports can significantly change the apparent damping of low-damping materials [20]. Therefore, we ensured consistent amplitude for the $1^{st}$ mode of each sample before the constant acceleration frequency sweep to provide comparable data. The tests were performed on the same beams that were used for LDM, testing two samples from a single plate that was removed and re-clamped until three repeat measurements were obtained for each sample, totalling six tests per material configuration.

The 3D transfer function $H(\omega)$ of a vibrating beam was obtained from the Fourier transform of the accelerometer input $X(\omega)$, divided by the Fourier transform of the output $Y(\omega)$.

$$H(\omega) = \frac{Y(\omega)}{X(\omega)} \tag{21}$$

For analysis and data processing, $H(\omega)$ was split into the gain and phase. The gain of this transfer function was converted to dB and the phase $\phi(\omega)$ was extracted from the argument of $H(\omega)$

$$|H(\omega)|[\mathrm{dB}] = 20\log_{10}(|H(\omega)|[-]) \quad \phi(\omega) = \arg(H(\omega)) \tag{22}$$

The vertical dimension of $H(\omega)$ (shaker direction) was used for dynamic analysis while the other two dimensions were investigated to ensure that torsion or transverse modes were not excited during our measurements. To extract the resonances $n$, $f_n$ for each beam was approximated using $\phi(\omega)$ because the phase at resonance is close to $90° + n180°$ with $n \in \mathbb{N}$ at each $n$ with a deviation in frequency corresponding to damping effects. The local maxima of $|H(\omega)|$ then determined the exact resonance frequency $f_n = \omega_n/(2\pi)$. From this maximum, the half power points $\omega_i$ with $i = h_1, h_2$, were extracted. These were then used to compute the mode $n$ dependent quality factor (11) and $\psi_{VBM_n}$

$$\psi_{VBM_n} = 2\pi\sqrt{1 - \frac{\left(2 - \frac{1}{Q_n^2}\right)^2}{4}} \tag{23}$$

To find the elastic modulus at each mode $E_{VBM_n}$, the Euler beam equation was used (12):

$$E_{VBM_n} = \frac{\rho A \omega_n^2}{\beta_n^4 I_x} \tag{24}$$

Shown in Table 2, the formulation of each method from the dynamic model to the elastic modulus $E$ and the definition of specific damping capacity $\psi$ is summarised.

## 4. Results

### 4.1. Logarithmic decrement measurement

The elastic modulus $E_{LDM}$ and the damping $\psi_{LDM}$ were measured for the CFRP and FFRP angle-ply laminates, as shown in Fig. 2, for the first two modes. The elastic modulus $E_{LDM}$ decreased with increasing $\pm\theta$ at both mode 1 and mode 2. In mode 1, $E_{LDM}$ varied from 168 GPa to 7 GPa for CFRP angle-plies 0° to 90° and from 32 GPa to 5 GPa for FFRP angle-plies 0° to 90°. The $E_{LDM_2}$ of 0° CFRP for mode 2, $E_{LDM_2} = 55$ GPa was lower than expected. This was likely due to the low torsional stiffness of the 0° CFRP and concurrently occurring excitation of the torsional mode before the $2^{nd}$ longitudinal mode. Thus the identification of mode 2 as per (13) was not appropriate for the 0° CFRP laminate.

The measured damping at mode 1 $\psi_{LDM_1}$ increased with increasing angle-ply orientation $\pm\theta$ and was consistent with previous work [21]. The CFRP damped with $\psi_{LDM_1}$ varying from 3.1% to 7.3% for the angle-ply range 0° to 90°. The FFRP damped notably

**Table 2**
Dynamic, elastic and specific damping capacity (SDC) $\psi$ models for each damping measurement method.

| Method | Dynamic model | Elastic modulus | SDC $\psi$ |
|---|---|---|---|
| LDM | $0 = m\ddot{x}(t) + c\dot{x}(t) + kx(t)$ | $\frac{\rho A(2\pi f_n)^2}{\beta_n^4 I_x}$ | $2\delta$ |
| DMA | $f(t) = m\ddot{x}(t) + (E' - iE'')x(t)$ | $\Re(\mathbf{E})$ | $2\pi\tan(\gamma)$ |
| VBM | $\frac{\delta^4 w}{\delta x^4} + \frac{\rho A}{E_{VBM} I_x}\frac{\delta^2 w}{\delta t^2} = \frac{F(x,t)}{EIx}$ | $\frac{\rho A\omega_n^2}{\beta_n^4 I_x}$ | $2\pi\sqrt{1 - \frac{\left(2 - \frac{1}{Q^2}\right)^2}{4}}$ |

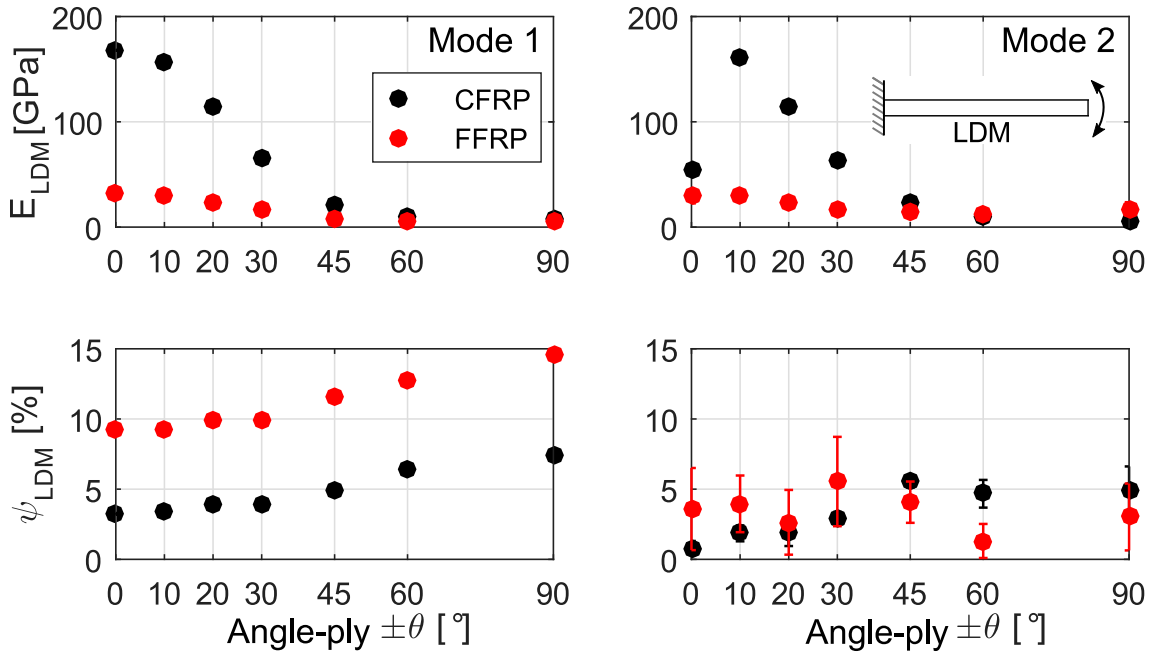


**Fig. 2.** Logarithmic decrement method (LDM) analysis of CFRP and FFRP as a function of angle-ply orientation $\pm\theta$ shows the elastic modulus $E_{LDM}$ and the specific damping capacity $\psi_{LDM}$ at the 1*st* and 2*nd* modes of vibration.

more and $\psi_{LDM_1}$ varied from 9.1% to 14.5% in the angle-ply range 0° to 90°. The value of $\psi_{LDM_1}$ for FFRP was approximately twice the magnitude of CFRP for all angle-ply orientations that were studied.

In mode 2 of vibration, the damping $\psi_{LDM_2}$ showed high variance and no clear correlation between $\psi_{LDM_2}$ and $\pm\theta$ for the studied materials. Since the $2^{nd}$ mode was excited much less than the $1^{st}$ mode, the Fourier spectra were much noisier, making identification of the peak in the data difficult.

### 4.2. Dynamic mechanical analysis

The elastic modulus $E_{DMA}$ was measured as 147 GPa to 7 GPa for CFRP angle-plies 0° to 90° at 1 Hz (Fig. 3 top). The DMA measured modulus for the 0° CFRP was found to be lower than the quasi-static flexural modulus of 195 GPa. The $E_{DMA}$ for FFRP measured as 29 GPa to 4 GPa for angle-ply orientations 0° to 90°, which were in the range of our measured quasi-static values. At 25 Hz, no

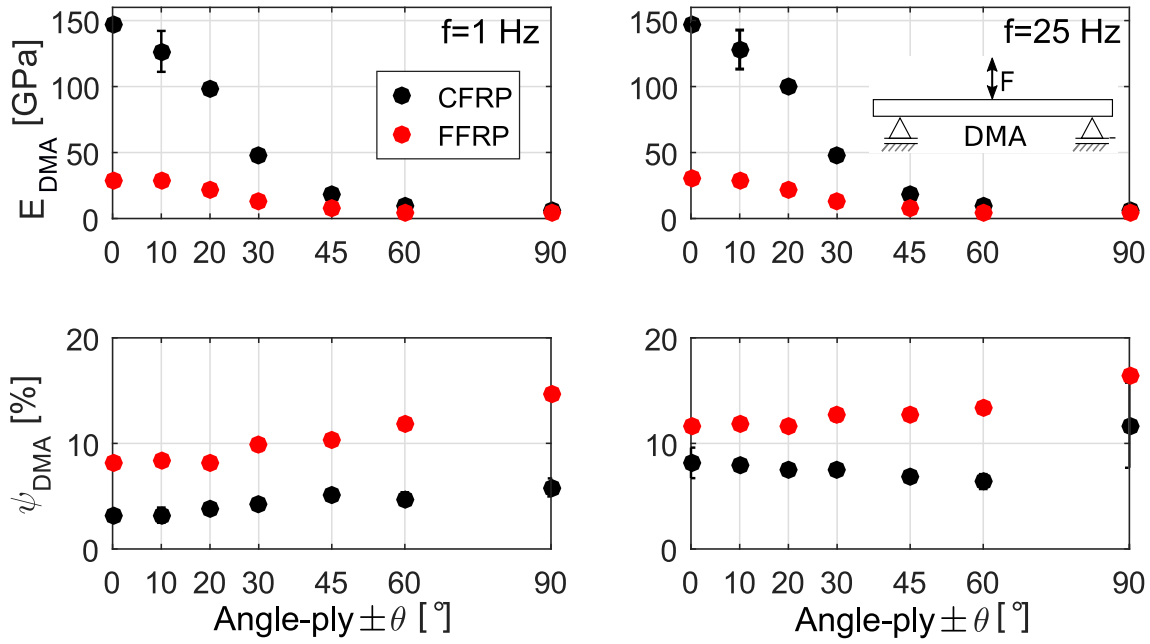


**Fig. 3.** Dynamic mechanical analysis (DMA) of CFRP and FFRP as a function of angle-ply orientation $\pm\theta$ shows the elastic modulus $E_{DMA}$ and the specific damping capacity $\psi_{DMA}$ at $f = 1$ Hz and 25 Hz.

difference in the value of $E_{DMA}$ was noted compared to the measurements at 1 Hz.

The value of $\psi_{DMA}$ increased with increasing angle-ply orientation for both materials (Fig. 3 bot.). For the 1 Hz CFRP measurements, $\psi_{DMA}$ increased from 3.0% to 5.6% with increasing angle-ply orientation. The value of $\psi_{DMA}$ for FFRP increased from 8.1% to 14.5% with increasing angle-ply orientation. The value of $\psi_{DMA}$ was about 2.5 times higher in FFRP compared to CFRP for the angle-ply orientations studied.

At 25 Hz, both composites damped more, notably at smaller angle-ply orientations. The value of $\psi_{DMA}$ varied from 7.9% to 11.5% and 11.4% to 16.3% for the CFRP and FFRP 0° to 90° angle-ply orientations, respectively. The increase with ply angle was notably flatter and an increased scatter in the data was observed.

### 4.3. Vibration beam measurement

Fig. 4 presents results for damping at different frequencies, by keeping the modal number constant in each of the plots, shown for the first four modes of vibration. For example, mode 1 occurred at frequencies in the range 42 Hz to 9 Hz or 19 Hz to 8 Hz for the CFRP and FFRP composites. At mode 4, these frequencies increased to 1639 Hz to 336 Hz or 733 Hz to 292 Hz, respectively, with the stiffer (closer to 0° orientations) having a higher natural frequency at each mode.

The elastic modulus $E_{VBM}$ varied as a function of angle-ply orientation for the measured modes of vibration, as shown in Fig. 4. Lower than expected values of $E_{VBM}$ were measured in mode 1, while modes 2 to 4 roughly follow classical laminate theory predictions. For example, $E_{VBM_2}$ varied from 142 GPa to 5 GPa and 33 GPa to 5 GPa for the CFRP and FFRP 0° to 90° angle-ply orientations respectively.

In mode 1, the measured $\psi_{VBM_1}$ for both materials was larger in magnitude than the other modes and was found to increase with angle-ply orientation until a maximum for the 90° composites. Since each beam measurement was conducted at a constant acceleration amplitude for a frequency sweep, the displacement amplitudes $X(\omega)/\omega^2$ at mode 1 were much higher than for other

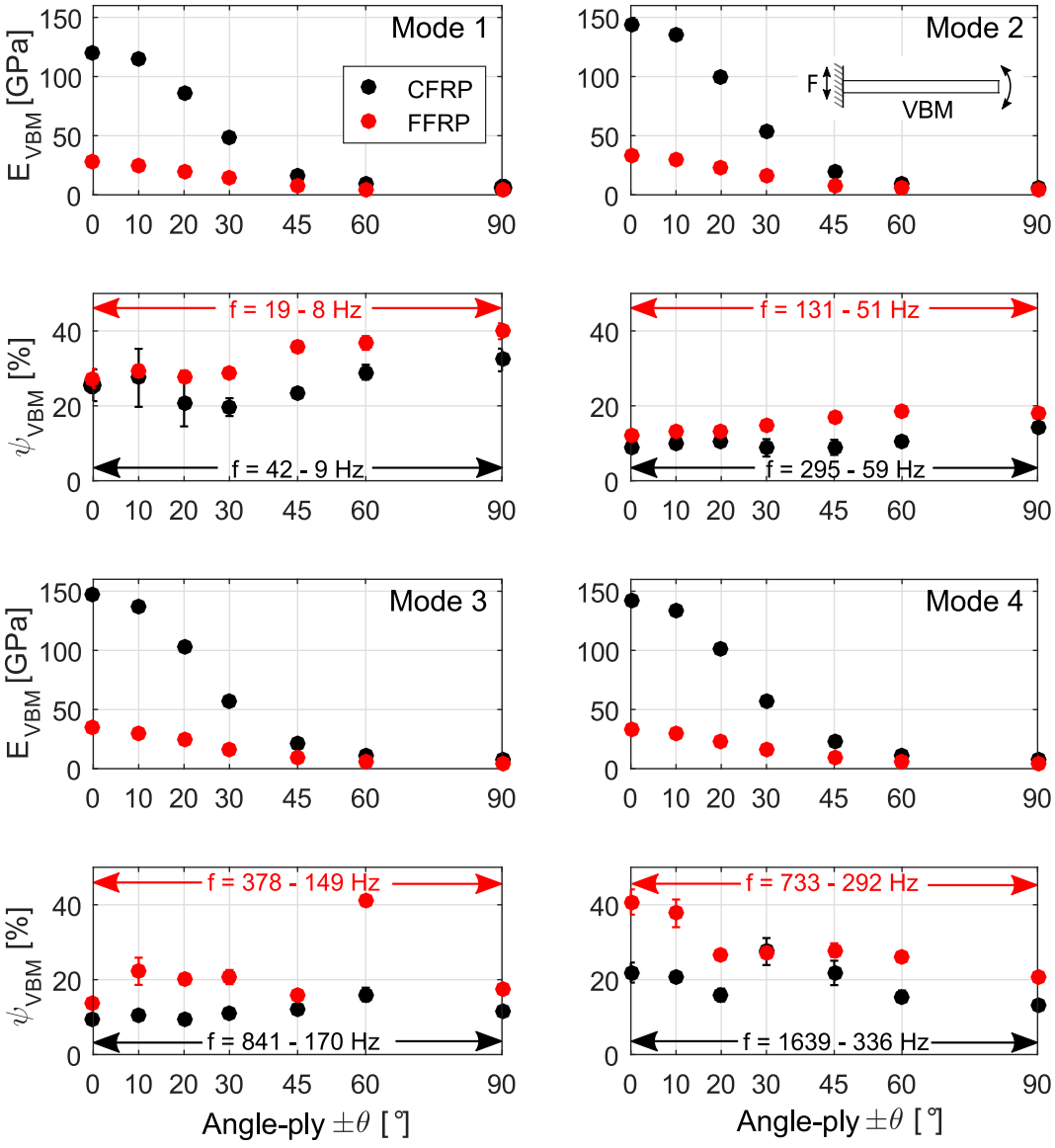


**Fig. 4.** Vibration beam measurements of CFRP and FFRP as a function of angle-ply orientation $\pm\theta$ shows the identified dynamic elastic modulus $E_{VBM}$ and the specific damping capacity $\psi_{VBM}$.

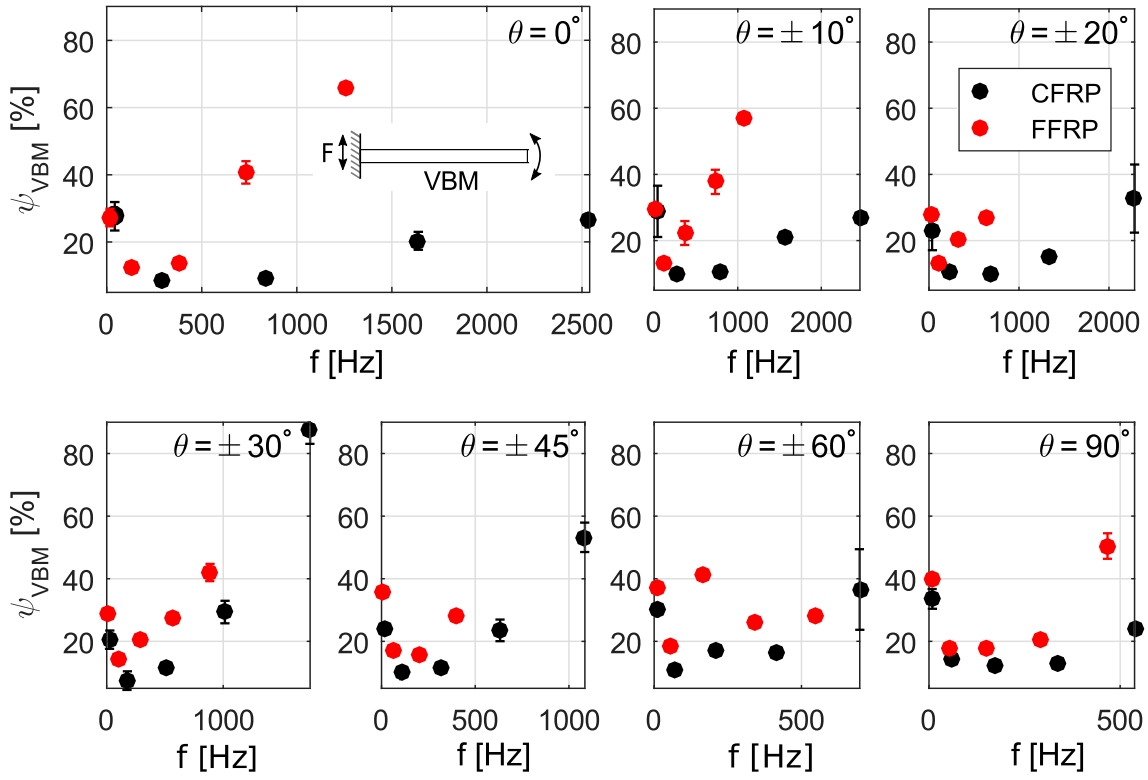


**Fig. 5.** Vibration beam measurements of CFRP and FFRP as a function of frequency shows the specific damping capacity $\psi_{VBM}$ for the studied angle-ply orientations $\pm\theta$.

measured modes. Air drag contributes to the damping for high amplitude tests [20] and therefore the measured resonance of a material is shifted to lower frequencies in the $1^{st}$ mode of vibration when air damping is prominent. For subsequent modes of vibration, tip displacements were much lower due to the modal shapes of the beams. Additionally, for the low $\pm\theta$ CFRP composites (the stiffest), compliance of the measurement set-up relative to the stiffness of the sample would cause low angle-ply CFRP $\psi_{VBM}$ in mode 1 to be larger than expected due to damping from the CFRP micro-structural architecture alone. This effect was noted in the CFRP $\psi_{VBM}$ for $\pm10^\circ$ and $\pm20^\circ$ in mode 1.

The $2^{nd}$ mode damping $\psi_{VBM_2}$ also increased with angle-ply orientation from 8.7% and 11.9% to a maximum of 13.8% and 17.6% at $\theta = 90^\circ$ for the CFRP and FFRP composites, respectively. The difference between $\psi_{VBM_2}$ for the $0^\circ$ and $90^\circ$ angle-ply orientations was less for both the studied composites. Mode 3 values of $\psi_{VBM}$ were found to peak for the $\pm60^\circ$ angle-ply orientations, being less pronounced for the CFRP ($\psi_{VBM_3} = 15.3\%$) than for the FFRP ($\psi_{VBM_3} = 40.8\%$) composites. In mode 4 of vibration, no obvious trend was observed for the CFRP composites. The FFRP however, presented highest damping at $0^\circ$ with $\psi_{VBM_4} = 40.1\%$, decreasing to $\psi_{VBM_4} = 20.3\%$ for the $90^\circ$ FFRP.

The damping $\psi_{VBM}$ versus the frequency $f$ for each angle-ply orientation was also compared, shown in Fig. 5. Each point indicates the magnitude of damping at the natural frequency for the first 5 modes of vibration. Below about 300 Hz, the difference in $\psi_{VBM}$ between CFRP and FFRP was small, but typically higher for the FFRP composites (upto a factor 2). With increasing frequency, an increasing deviation between the value of $\psi_{VBM}$ for the two materials was noted. For the $90^\circ$ composites, little difference was observed in the value of $\psi_{VBM}$, with strong deviation only observed in the $5^{th}$ mode, when the FFRP experienced much more damping than the CFRP (47.5% versus 19.6%). The tendency of increasingly higher damping in FFRP was more prominent as the angle-ply orientation approached $0^\circ$ (i.e. the fibre direction). The value of $\psi_{VBM}$ for the FFRP $0^\circ$ was measured as $\psi_{VBM_5} = 65.4\%$ while maintaining stiffness.

## 5. Discussion

The elastic moduli $E_{VBM}$ showed no strong frequency dependence up to the $5^{th}$ mode using the vibration methods that were studied. While CFRP composites are known to demonstrate rate sensitivity in $E_{VBM}$, data for CFRP and FFRP were both rather independent of frequency up to 2.5 kHz. Limitations in the elastic modulus identification were noted for the stiffest samples, such as for $0^\circ$ CFRP. The value of $E$ for those samples were measured with LDM as 168 GPa, with DMA as 147 GPa and with VBM as 143 GPa, which were all lower than the measured 195 GPa from quasi-static bending tests. Clamping of the LDM and VBM testing set-ups or the relative short span of the DMA three point bending was believed to be the main cause of this discrepancy, which would have the effect of elevating the measured values of $\psi$ beyond contribution to the CFRP only, at low values of $\pm\theta$. The elastic moduli for $0^\circ$ FFRP were identified with LDM at 32 GPa, with DMA at 29 GPa and with VBM at 31 GPa. Noting that FFRPs have a bilinear strain dependent elastic modulus with transition at approximately 0.2% strain [22], the identified elastic modulus showed good agreement with the measured bending elastic modulus of 31 GPa.

### 5.1. Damping of carbon fibre and flax fibre reinforced polymer composites

The two composite materials were compared using LDM mode

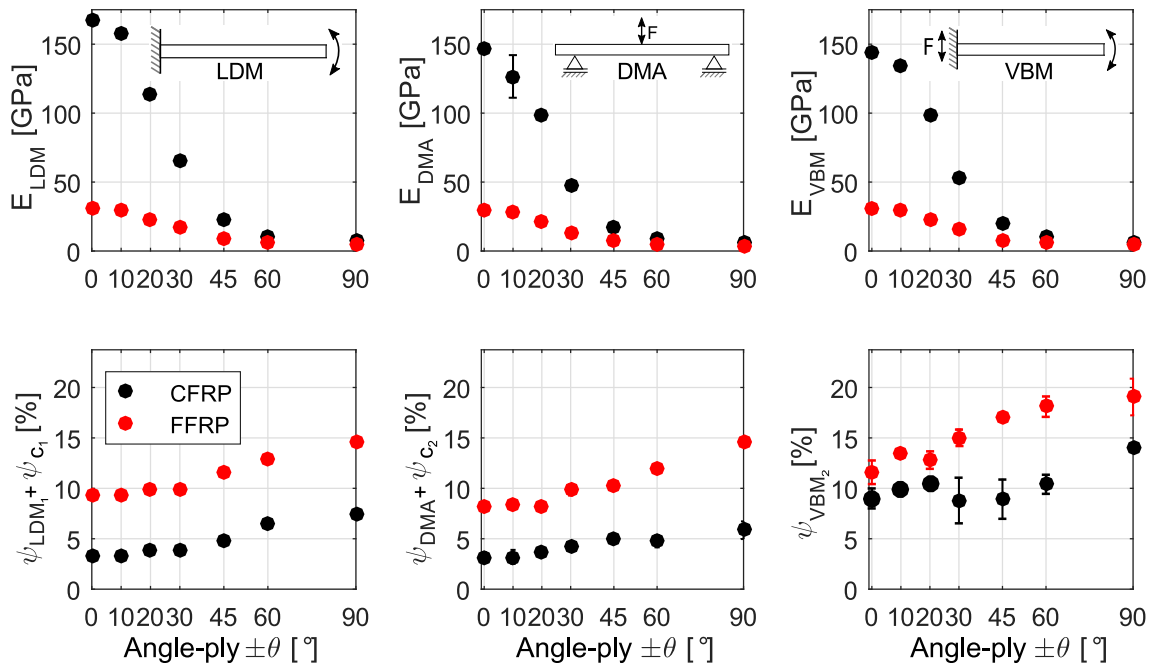


**Fig. 6.** Comparison of the elastic modulus $E$ and the specific damping capacity $\psi$ of CFRP and FFRP as a function of angle-ply orientation $\pm\theta$ using the 1*st* mode of the logarithmic decrement method (LDM), dynamic mechanical analysis (DMA) measurements at 1 Hz and the 2*nd* mode of the vibration beam method (VBM).

1, DMA at 1 Hz, and VBM mode 2 results. The value of $\psi$ was lowest for the CFRP at 0° and highest at 90°, which is consistent with previous work [21]. The FFRP composites were measured to have two to three times higher $\psi$ than CFRP. The measurements for $\psi_{VBM}$ (Fig. 5), were found to increase with frequency from the lowest value of $\psi_{VBM}$ in mode 2. For the angle-ply range $0° - \pm 30°$, the rise in $\psi_{VBM}$ was also increasingly larger in magnitude in the FFRP compared to the CFRP composites.

This shows that both materials are frequency dependent and that the angle-ply orientation plays a crucial role for optimal damping at frequencies above approximately 300 – 400 Hz. The FFRP composites demonstrated vibration suppression while maintaining a high specific stiffness. This suggests that the hierarchical fibre micro-structure of flax fibres strongly contributes to damping at higher frequencies. Some of the notable results include $\psi = 47.8\%$ at 472 Hz for the 90° FFRP and the highest damping of $\psi_{VBM_5} = 65.4\%$ at 1259 Hz in the $5^{th}$ mode for the 0° FFRP composite in the fibre direction.

### 5.2. Comparison of measurement methods

The LDM measurements were performed on fixed cantilever samples, meaning some additional damping due to the clamp mass and friction at the mount would have been present. However, with relatively low frequencies of vibration of excitation and small amplitudes (maximum of 300 Hz and 10 mm tip displacement), little additional damping due to air resistance would have occurred. The DMA measurements were performed clamp-free, with a small coupon at a frequency of 1 – 25 Hz, creating little air drag due to the low frequency and amplitude of oscillation (up to 42 $\mu$m). The same clamping set up was used for samples tested by VBM as LDM, but as the amplitude of vibration was larger during VBM, air resistance effects on the damping were more prominent; especially for mode 1 with beam tip amplitudes up to 150 mm.

Interestingly, the data for $\psi$ versus $\pm\theta$ for the studied methods presented consistent trends, albeit at different magnitudes of $\psi$. Likewise $E$ versus $\pm\theta$ compare reasonably well, with deviations only at the lowest CFRP angle-ply orientations. To attempt to compare the methods, damping results from the LDM, DMA and VBM were least squares fitted to quantify the damping effects caused by the measurement method. The $1^{st}$ mode of the $\psi_{LDM}$, $\psi_{DMA}$ at 1 Hz and the 2*nd* mode of $\psi_{VBM}$ (to have a VBM measure with less air damping and the same bending modal shape at the DMA tests) were compared

$$\psi_{LDM_1} + \psi_{c_1} = \psi_{DMA} + \psi_{c_2} = \psi_{VBM_2} \tag{25}$$

using the constant damping term $\psi_{c_i}$.

The constant external damping $\psi_{c_1} = 0.8\%$ and $\psi_{c_2} = 5.10\%$ can be interpreted as damping due to external effects such as air resistance and clamping effects in the VBM measurements, respectively. Shown in Fig. 6, the results compare well quantitatively, demonstrating that $\psi$ could be useful when comparing across methods, however noting that it is important to quantify external effects and to understand the limitations of each test methodology when comparing data using the different methods.

## 6. Conclusions

This paper describes three damping measurement tests for continuous fibre reinforced polymer composites and develops a methodology to compare across sample size, excitation frequencies and applied strain. Our methodology was used to study carbon fibre and flax fibre reinforced composites. It was possible to compare across the LDM, DMA and VBM measurement methods using the specific damping capacity $\psi$ despite the methodologies being rather different.

Notably, the LDM provided non-linear decay for both the materials, suggesting that one must carefully consider initial parts of the displacement curve during tests to identify the two vibrating

frequencies that were observed. For materials with high damping, the LDM method in time domain can provide useful data [4] due to the quick decline of $f_2$ and large magnitude of $\tau_2$. However, the identification can be difficult since the decline contains a superposition of more than one exponential decline, especially at the initial moment of the vibration. The DMA provided useful information about the materials at low strain and relatively low frequencies. A large range of amplitudes and frequencies may be studied using VBM, meaning FFRP could be characterised in a variety of strain conditions and a number of natural frequencies. We noticed that additional damping through air resistance occurred due to the large amplitudes of vibration, especially in the $1^{st}$ mode.

By using CFRP as a reference material, we studied hierarchically structured FFRP composites. The FFRP composites consistently damped about 2–3 times more than the CFRP composites at a given angle-ply orientation at low frequencies and low strains. Both materials followed the same trend with respect to angle-ply orientation, albeit larger in magnitude for the FFRP composites. We found that above $300 - 400$ Hz, highest damping occurs evermore closer to the fibre direction as the frequency increases. The unidirectional FFRP was found to have $\psi = 65.4\%$ of energy per cycle dissipated in vibration suppression, at frequencies of 1259 Hz in the $5^{th}$ mode without a change in the elastic modulus. Such composites could be extremely valuable because damping can be incorporated via micro-structures in the reinforcing fibre.

## Acknowledgements

This work was carried out in the research project TWiCDamp funded by the Swiss Space Office, grant agreement no. 236-01D3/Bro and ETH Foundation grant SP-MaP 01-15, within the framework of the Swiss Competence Center for Energy Research (Capacity Area A3: Minimization of energy demand). The contributions of W. Woigk, L. Repond, and F. Stork are gratefully acknowledged, as well as Prof. H-P. Gröbelbauer for use of the shaker.

## References

[1] C. Baley, Analysis of the flax fibres tensile behaviour and analysis of the tensile stiffness increase, Compos. Part A - Appl. Sci. Manuf. 33 (2002) 939–948.
[2] K. Oksman, A. Mathew, R. Långström, B. Nyström, K. Joseph, The influence of fibre microstructure on fibre breakage and mechanical properties of natural fibre reinforced polypropylene, Compos. Sci. Technol. 69 (2009) 1847–1853.
[3] B. Madsen, M. Aslan, H. Lilholt, Fractographic observations of the microstructural characteristics of flax fibre composites, Compos. Sci. Technol. 123 (2016) 151–162.
[4] F. Duc, P. Bourban, J. Manson, The role of twist and crimp on the vibration behaviour of flax fibre composites, Compos. Sci. Technol. 102 (2014) 94–99.
[5] M. Rueppel, J. Rion, C. Dransfeld, K. Masania, Damping of carbon fibre and flax fibre reinforced angle ply polymers, in: Proceedings of ECCM17-17th Euro. Conf. on Compos. Mater., Munich.
[6] H. Kishi, M. Kuwata, S. Matsuda, T. Asami, A. Murakami, Damping properties of thermoplastic-elastomer interleaved carbon fiber-reinforced epoxy composites, Compos. Sci. Technol. 64 (2004) 2517–2523.
[7] R. Chandra, S.P. Singh, K. Gupta, A study of damping in fiber-reinforced composites, J. Sound. Vib. 262 (2003) 475–496.
[8] R.S. Lakes, High damping composite materials: effect of structural hierarchy, J. Compos. Mater 36 (2002) 287–297.
[9] D.J. Nelson, J.W. Hancock, Interfacial slip and damping in fibre reinforced composites, J. Mater. Sci. 13 (1978) 2429–2440.
[10] S. Vengallatore, Analysis of thermoelastic damping in laminated composite micromechanical beam resonators, J. Micromech. Microeng. 15 (2005) 2398–2404.
[11] M. Maheri, R. Adams, Steady-state flexural vibration damping of honeycomb sandwich beams, Compos. Sci. Technol. 52 (1994) 333–347.
[12] J.Y. Lai, K.F. Young, Dynamics of graphite/epoxy composite under delamination fracture and environmental effects, Compos. Struct. 30 (1995) 25–32.
[13] L. Gaul, J. Lenz, Nonlinear dynamics of structures assembled by bolted joints, Acta Mech. 125 (1997) 169–181.
[14] F. Guild, R. Adams, A new technique for the measurement of the specific damping capacity of beams in flexure, J. Phys. E 14 (1981) 355–363.
[15] R. Amacher, J. Cugnoni, J. Botsis, L. Sorensen, W. Smith, C. Dransfeld, Thin ply composites: experimental characterization and modeling of size-effects, Compos. Sci. Technol. 101 (2014) 121–132.
[16] C.W. Bert, Material damping: an introductory review of mathematic measures and experimental technique, J. Sound. Vib. 29 (1973) 129–153.
[17] K.K. Chawla, Interfaces in Composite Materials: Science and Engineering, Springer Science and Business Media, New York, NY, 2012.
[18] M. Carfagni, E. Lenzi, M. Pierini, S. Marta, The loss factor as a measure of mechanical damping, in: Proceedings-spie the International Society for optical Engineering, pp. 580–584.
[19] D.J. Ewins, S. Braun, S. Rao, Beams, Encyclopedia of Vibration, vol. 1, Academic Press Ltd, 2001.
[20] M. Maheri, R. Adams, Vibration properties of structural FRP composites, JSME Int. J. Ser. A Solid Mech. Mater. Eng. 42 (1999) 307–320.
[21] R. Adams, M. Maheri, Dynamic flexural properties of anisotropic fibrous composite beams, Compos. Sci. Technol. 50 (1994) 497–514.
[22] C. Baley, A. Le Duigou, A. Bourmaud, P. Davies, Influence of drying on the mechanical behaviour of flax fibres and their unidirectional composites, Compos. Part A Appl. Sci. Manuf. 43 (2012) 1226–1233.